Surface Energetics of Carbon Fibers and Its Effects on the Mechanical Performance of CF/EP Composites

F. HOECKER and J. KARGER-KOCSIS*

Institut für Verbundwerkstoffe GmbH, University of Kaiserslautern, P.O. Box 3049, D-67653 Kaiserslautern, Germany

SYNOPSIS

To exploit the reinforcement potential of the fibers in advanced composites, it is necessary to reach a deeper understanding on the interrelations between fiber surface chemical and energetic characteristics, wetting properties, and mechanical performance. In this study CF/EP was chosen as a model thermoset composite material, whereby a hot-curing epoxy (EP) system served as the matrix. The fibers selected were PAN-based high-tenacity carbon fibers (CF) of varying surface treatment level and/or coating. Surface free energies for the carbon fibers were determined by dynamic contact angle measurements in a variety of test liquids of known polar and dispersive surface tension utilizing a micro-Wilhelmy wetting balance and following the methods proposed by Zisman and Owens and Wendt, respectively. Surface treatment resulted in an increase of the polar fraction of the fiber surface free energy, whereas its dispersive part remained unaffected. The interfacial shear strength (IFSS) as determined in the microdroplet pull-off test was enhanced both by intensification of the surface treatment and sizing the CF with an EP component. A linear relationship between IFSS and the polar fraction of the fiber surface free energy γ_s^p was found. Further attempts were made to find correlations between surface free energy of the CF and laminate strengths measured in shear and transverse tension.

INTRODUCTION

The mechanical performance of composites is determined mainly by the composition and arrangement of their constituents, i.e., matrix and reinforcement, involving parameters such as fiber volume fraction, fiber aspect ratio, fiber orientation, as well as strength and moduli of matrix and fibers, respectively. Considering the volume-related contact surface of the fibers (6–10 μm in diameter) being in the range of 10^5 to 10^6 m^2/m^3 for advanced composite materials (fiber volume fraction 40–60%),[1] the dominant role of the interface becomes obvious. To utilize the full potential of the reinforcing fibers, both perfect impregnation (or wetting) and formation of strong bonds have to be guaranteed for reliable materials in structural applications. On the other hand, a weak interfacial link providing increased toughness by promotion of pull-out effects can be desirable and beneficial for energy-absorption purposes, e.g., crash elements for bumpers. Therefore, even "interface-tailoring" upon strength/stiffness and/or toughness requests seems not to be unrealistic, but this can only happen based on a comprehensive knowledge of the nature and characteristics of the interface.

The adhesive bond itself may, in principle, be due to chemical (covalent), physical (including acid–base type), or mechanical (interlocking or anchoring) interactions across the interface. Adhesion phenomena are not only very complex, but they are also not fully understood yet from a scientific point of view. So, in respect to carbon fibers (CF) and epoxy resin (EP), one has, e.g., to take into account (a) both the microstructure and chemistry of the CF surface and (b) possible reactions of the matrix components (resin + curing agent) with functional groups at the CF surface.[2,3]

When CFs first became available, the bonding between the fibers and the matrix resins used was poor.[4] This fact relies on the heterogeneous buildup of CF consisting of layered aromatic planes (plate-

* To whom correspondence should be addressed.

Journal of Applied Polymer Science, Vol. 59, 139–153 (1996)
 CCC 0021-8995/96/010139-15

lets).[5] The various structural models for CF have been reviewed by Hüttinger et al.[2] The "classical" description (see Fig. 1) shows differences in the degree of orientation of platelets in the core and skin regions (the latter having a more ordered structure with preferred orientation parallel to the fiber surface[5]). Considering the chemically potential active sites on a graphite crystal that may contribute to adhesion, they can be found on edges of the basal planes, structural imperfections, or lattice defects.[6] The basal crystal surfaces of fully bonded carbon atoms are chemically inert. Therefore, the reactivity of a CF is greatly dependent on the (dis)order of its structure; in other words, the more graphitic and aligned the surface, the less is the affinity for chemical bonding.[7] That is the reason why all commercial CFs are available in surface-treated form. In principle, all the proprietary surface treatments, i.e., dry gaseous, wet chemical, electrolytic (anodic), or plasma treatment oxidation processes, are of an oxidative nature.[7] As a result, four major possible mechanisms contributing to the fiber/matrix bond are triggered: (i) removal of surface contaminants which may inhibit wetting of the fiber or block active sites; (ii) removal of weak boundary layers, providing a mechanically sound surface which the resin molecules can adhere; (iii) microroughening of the surface to increase contact area and promote mechanical anchoring effects; and (iv) production of chemically or physically active sites (owing to the attack of faulty surface areas in the basal planes) to bond with the polymer matrix.[1,4,8]

During recent years, extensive research activities have been devoted to the question of which one of the above-listed mechanisms is responsible for an increased fiber/matrix bond strength for surface-treated CFs. Nevertheless, the results are contradictionary: In particular, it is not clear whether the chemical bond on its own is the relevant and dominating mechanism in CF/EP composites. Interested readers on this topic are addressed to Refs. 3, 4, 6, and 9–13. In summary, all the articles agree that (i) in most cases an increase in the surface functionality (oxygen-containing functional groups) is accompanied by an increase in surface area, which makes the differentiation of these two factors difficult.[7,12] Whatever type of surface treatment is used, the number of chemical bonds is limited by the number of reactive sites available ("active surface area"). The active surface is controlled by the physical structure of the fiber (graphitization and orientation) and its microtopography.[7] (ii) The main functional groups produced by standard surface-treatment techniques are carboxyl (COOH), carbonyl (CO), and hydroxyl (OH),[4,6] all of acidic nature. The strongly acidic carboxylic groups exhibit a stronger interaction with materials of alkalic character than the other groups present on the CF surface and thus are the ones principally responsible for adhesion to basic polymers.[14] In general, it can be stated that improvements in the adhesion will always depend on both the fiber and matrix material used and on the particular surface treatment applied.

A surface treatment process generally consists of a surface cleaning (and activating) step which may be followed by the application of a "finish," "coupling," or "compatibility" coating or sizing.[1] The intended function of this size, i.e., usually an epoxy without a hardener for EP matrices, is to improve the handling of the tow and to decrease surface

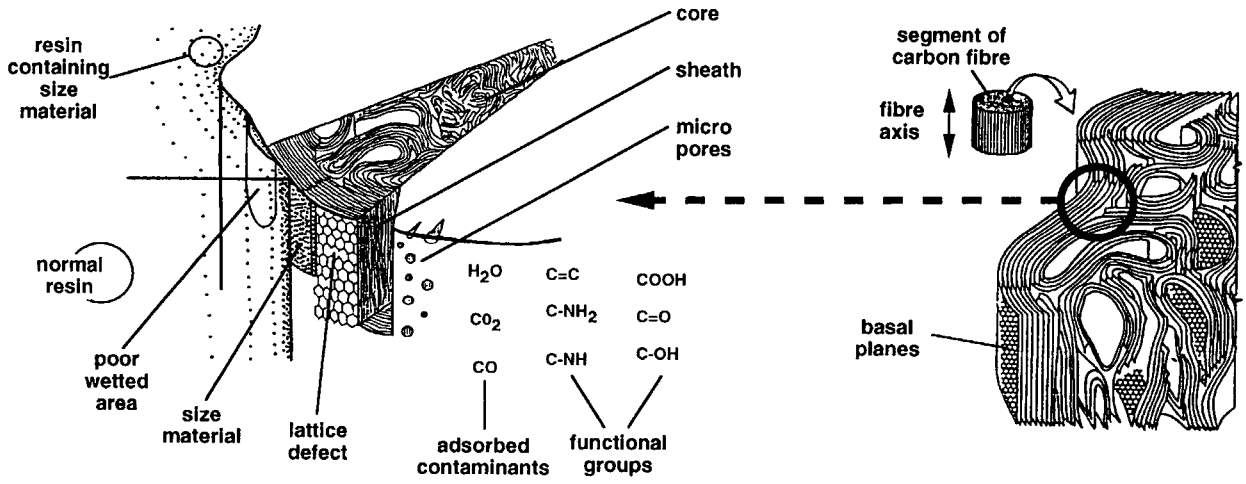

Figure 1 Structure model of PAN-based high-tenacity (type II) CFs and interphase after Refs. 5 and 6.

damage to the fibers during industrial operations. Although controversially discussed, it has been reported that the presence of a finish may improve the wetting performance of the fiber by the matrix resin and protect its surface reactivity.[4,7,15] It was also suggested that the structure of the sizing resin and even its deposition technique affects the wetting.[16,17] The effect of hydrogen bridging and even of stable covalent bonds with surface active groups has been found to be responsible for the wetting performance.[6,12] Anyway, the presence of sizings or coatings on CFs suggests that the interphase (which exists in three dimensions) concept is correct rather than the interface (two-dimensional) approach. As it is dissimilar to the bulk matrix material in stoichiometry and thus mechanical properties,[18] it may affect essentially the mode of failure in composites.[15] A variety of more or less complex schemes on such interphases is proposed in the literature, e.g., by Drzal[9,15] and Hughes,[7] but the most comprehensive model is given by Matsui[6] (see Fig. 1). Here, not only active surface sites and matrix functional groups are considered, but also sizing, adsorbants, and wetting performance are taken into account.

Adhesion between fiber and matrix cannot be achieved without intimate contact, i.e., unless the fiber surface contacts the resin on a molecular level.[6] Then, the molecules will undergo motions toward preferred configurations to reach an absorptive equilibrium. This results in the formation of a diffuse interphasial zone and/or chemical bonds across the interface.[19] Thermodynamic wetting is thus a necessary but not a sufficient prerequisite for adhesion. It was the aim of this study to correlate fiber surface properties to the mechanical properties of composites in both micromechanical and macromechanical scale.

THEORETICAL CONSIDERATIONS

Thermodynamics of Wetting

When a drop of liquid comes into contact with an ideally smooth, homogeneous, planar, and nondeformable surface, either a thin wetting film or a drop under a finite angle forms on the solid surface. This three-phase equilibrium boundary among the solid, liquid, and vapor is described by Young's equation that relates the static contact angle θ to the various interfacial tensions (see Fig. 2):

$$\gamma_{lv} \cos \theta = \gamma_{sv} - \gamma_{sl} \tag{1}$$

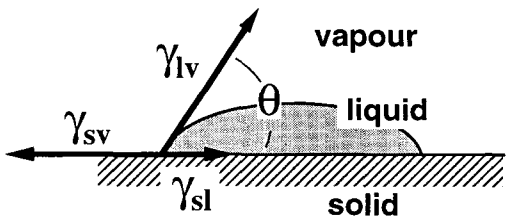

Figure 2 Force equilibrium for a sessile drop.

where γ_{lv}, γ_{sv}, and γ_{sl} are the interfacial free energies of the liquid/vapor, solid/vapor, and solid/liquid interface, respectively.

The contact angle is used as a measure of the degree of attraction of the liquid for the substrate. If the contact angle is 0° or less than 90°, the liquid is said to spread on or to wet the substrate, respectively. If it is greater than or equal 90°, the liquid/solid interaction is termed to be nonwetting.

Adsorption of a vapor on a liquid or on a solid will change the surface tension of this substrate. Generally, adsorption will occur when the condensed vapor has a surface tension similar to or lower than the substrate. The equilibrium spreading pressure of the vapor on the substrate π_e is defined as

$$\pi_e = \gamma_S - \gamma_{Sv} \tag{2}$$

where γ_S stands for the surface tension (or surface free energy) of the substrate (solid or liquid) in vacuum and γ_{Sv} is its interfacial tension in equilibrium with the saturated vapor of the wetting liquid.[19]

When a liquid absorbs its own vapor phase, its surface tension will remain unchanged, i.e., $\gamma_{lv} = \gamma_l$. For relatively low energy solids, there is negligible adsorption of the liquid vapor phase onto the solid surface, π_e diminishes, and $\gamma_{sv} = \gamma_s$.[20] Therefore, eq. (1) may be rewritten:

$$\gamma_l \cos \theta = \gamma_s - \gamma_{sl} \tag{3}$$

The thermodynamic work of adhesion (W_a) is also a measure of the interaction between two phases, i.e., the greater the work of adhesion, the greater the interfacial attraction. It is given by the work required to separate reversibly the interface between two phases from their equilibrium to infinity, i.e., for generating the solid/vapor and the liquid/vapor interfaces (>0) and eliminating the solid/liquid interface (<0). This energy balance is given by Dupré's equation:

$$W_a = \gamma_s + \gamma_l - \gamma_{sl} \tag{4}$$

Inserting Young's equation [eq. (3)], W_a is given by the Young–Dupré equation:

$$W_a = \gamma_l(1 + \cos\theta) \tag{5}$$

The various molecular attractive forces are assumed to be linearly additive. Both the work of adhesion and the surface tension can, therefore, be separated into two terms[19]:

$$W_a = W_a^d + W_a^p \tag{6}$$

$$\gamma = \gamma^d + \gamma^p \tag{7}$$

where the superscript d refers to the contribution due to London dispersion forces which are common to all materials, while p relates to the Keesom polar contribution, largely made up of hydrogen bonding and dipole–dipole interactions.[20] So, the total surface free energy of the solid surface and the liquid can be simply expressed by $\gamma_s = \gamma_s^d + \gamma_s^p$ and $\gamma_l = \gamma_l^d + \gamma_l^p$. The interfacial tension between the solid and the liquid is assumed to be equal to the geometric mean,[19] i.e.:

$$\gamma_{sl} = \gamma_s + \gamma_l - 2(\gamma_s^d\gamma_l^d)^{1/2} - 2(\gamma_s^p\gamma_l^p)^{1/2} \tag{8}$$

Similar equations were also proposed empirically by Owens and Wendt[21] and Kaelble et al.[22] When the polar term is neglected, eq. (8) is known as the Fowkes equation.[23]

Although the harmonic mean approach is reported to be superior in predicting the interfacial tensions of polymers and low-energy materials,[19] the geometric mean method has been successfully applied for surface treated CF substrates, e.g., by Hammer and Drzal.[24] By substitution of γ_{sl} in Dupré's eq. (4) by eq. (8), the work of adhesion with its dispersive and polar components becomes

$$W_a = 2[(\gamma_s^d\gamma_l^d)^{1/2} + (\gamma_s^p\gamma_l^p)^{1/2}] \tag{9}$$

Fiber Surface Free Energy Analysis

Surface energetic analyses of fibrous materials are based on the determination of contact angles in wetting studies with liquids of known surface tensions. In general, contact angles can be determined either directly by optically observing the shape of a liquid droplet attached to a monofilament (e.g., Ref. 20) or indirectly via measurement of the force required to immerse (or emerse) a single monofilament into (or from) a liquid of known surface tension at constant velocity (e.g., Ref. 24). However, the measurement of contact angles for the wetting of cylindrical filaments of the order of 10 μm requires a more sophisticated approach than is necessary for simple planar surfaces.

Critical Surface Tension

The concept of critical surface tension γ_c was first proposed by Zisman[25] who found a linear relation between the cosinus of measured contact angles θ and (known) γ_l for a series of homologous testing liquids on a solid. When nonhomologous liquids are used, however, the data are often scattered.[19] The so-called Zisman plot shows cos θ vs. γ_l, where the intercept of the line at cos $\theta = 1$ is identified as the critical surface tension γ_c. The critical surface tension equals the total surface free energy γ_l^* of the liquid which just spreads on the solid, i.e., that just exhibits a zero contact angle. Referring to Young's equation,

$$\gamma_l^* = \gamma_c = \gamma_s - \gamma_{sl} \tag{10}$$

It is indicated that γ_c is smaller than γ_s by the amount of γ_{sl}. Furthermore, the spreading pressure π_e is not taken into account. Therefore, γ_c will vary with the testing liquids used and tends to be more or less smaller than γ_s.[19] In summary, γ_c values must be used with caution.

Polar/Dispersive Surface Free Energy Analysis

Combining eq. (9) with eq. (5) yields, in accordance to Owens and Wendt[21] and Kaelble et al.,[22] a linear equation in the form of $y = mx + b$ with the slope "m" and intercept "b" given by the square root of the polar and dispersive components of the solid surface free energy, such as

$$\frac{\gamma_l(1 + \cos\theta)}{2\sqrt{\gamma_l^d}} = \sqrt{\gamma_s^p}\left(\frac{\sqrt{\gamma_l^p}}{\sqrt{\gamma_l^d}}\right) + \sqrt{\gamma_s^d} \tag{11}$$

where γ_l, γ_l^d, and γ_l^p have to be known for the test liquids used to contact the surface of interest and the apparent contact angle θ is measured.

Wetting and Adhesion

From the theoretical point of view, wetting can affect adhesion in two ways: First, incomplete wetting will produce interfacial defects and thereby lower the adhesive bond strength by flaw-induced stress concentrations. Second, better wetting can enhance the adhesive bond strength by increasing the thermo-

dynamic work of adhesion, which is directly proportional to the fracture energy of the adhesive bond. However, these two models are not always compatible.[19]

Wetting and Interfacial Defect

Due to local material inhomogeneities, random microscopic voids and flaws may arise during wetting of a substrate by an adhesive. The driving force for the wetting of these defect sites is the spreading coefficient λ_{sl} of a liquid (adhesive) on a solid (adherend)[19]:

$$\lambda_{sl} = \gamma_l - \gamma_s - \gamma_{sl} \tag{12}$$

On the base of linear-elastic fracture mechanical considerations, in particular, the Griffith criterion for adhesive fracture under plane stress conditions, and assuming that the average size of an unwetted interfacial defect is related to λ_{sl}, Wu[19] proposed that wettability is directly related to the mechanical strength σ_f of an adhesive bond as follows:

$$\sigma_f = \frac{K_m \gamma_s}{\gamma_l + \gamma_{sl}} \tag{13}$$

where K_m is a function of the mechanical properties of the system taking into account Young's modulus E and fracture energy G, i.e., the energy required to separate one unit interfacial area. For a given adhesive on a series of adherends, γ_l remains unchanged, further providing that the mechanical parameter K_m is constant and assuming that $\gamma_l \gg \gamma_{sl}$, $\sigma_f \sim \gamma_s$. Therefore, eq. (13) may be rewritten as

$$\sigma_f = K(\gamma_s^p + \gamma_s^d), \tag{14}$$

or, by using eq. (5) for γ_s as

$$\sigma_f = K_1(1 + \cos\theta) + K_2 \tag{15}$$

where K, K_1, and K_2 are constants.

Wetting and Fracture Energy

As pointed out by Wu,[19] the fracture energy is directly proportional to the work of adhesion and given as the sum of thermodynamic work and work for local material plasticization. Since the latter contribution is a viscoelastic quantity, the fracture energy on the whole is dependent on rate, temperature, and loading mode. At zero-rate, viscoelasticity effects are diminishing, the separation process will be reversible, and the equilibrium fracture energy is equal to the work of adhesion. Thus, the adhesive bond strength should increase with increasing work of adhesion. Again, for a given adhesive on a series of adherends, viscoelasticity contributions should be similar, and the adhesive bond strength should therefore be proportional to the work of adhesion.[19]

EXPERIMENTAL

Materials

As a model thermoset matrix material, a hot-curing epoxy (EP) system (bisphenol-A-based resin Araldit LY 556; anhydride hardener HY 917, 90 phr; heterocyclic amine catalyst DY 070, 1 phr; all of them from Ciba, Basel, Switzerland; curing cycle: 4 h/80°C + 8 h/120°C) was selected. To determine the effect of surface treatment and sizing on both the individual fiber-surface properties and the mechanical performance of composites, two series of PAN-based high-tenacity carbon fibers (CF), each of them of one batch and only varying in the surface treatment and/or kind of sizing, were chosen: The fibers supplied by Idemitsu Kosan (Chiba, Japan) only varied in the intensity of surface treatment, i.e., "no," "mild," "usual," and "severe" levels, whereas the standard surface-treated types provided by Tenax Fibers (Wuppertal, Germany) did in their surface finish. The designations "HTA 5001," "HTA 5131," and "HTA 5411" stand for standard surface treatment and no sizing, 1.25 wt % EP-sizing, and 0.15 wt % antistatic agent, respectively. As a reference, the non-surface-treated and unsized "HTA 5000" was used. In addition to these modifications, "HTA 5411B" indicates coating of the standard-treated 5411 version with a high-temperature resistant mold release agent, Acmosan 82-60, provided by Acmos Chemicals (Bremen, Germany).[26] The fiber diameter was determined by scanning electron microscopy (SEM) for all types to be 7 μm. Since only the standard surface-treated Tenax types were available in a scale sufficient for manufacturing composite laminates and tubes, the macromechanical test methods were confined to the HTA 5411B, HTA 5411, and HTA 5131/EP systems.

Wetting Studies

Test Liquids

The total surface free energies γ_l of all test liquids to be used in the fiber wetting studies (bromonaphthalene, formamide, glycerine, distilled water, and

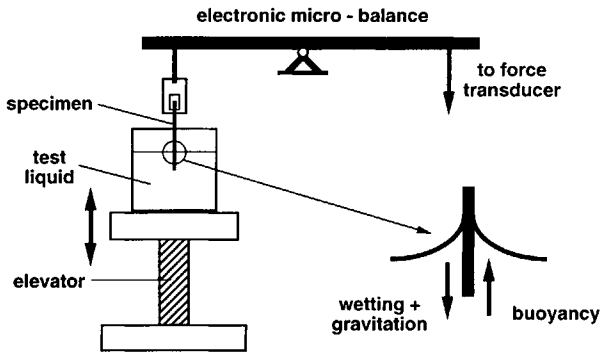

Figure 3 Schematic of a micro-Wilhelmy balance.

an ethylene glycol/formamide mixture) were determined following both the Wilhelmy plate (5 mm/min) and the DuNouy ring (1 mm/min) methods. These techniques are described and reviewed, e.g., in [19]. Experiments were performed using the Sigma 70 surface tension/contact angle meter of KSV Instruments (Helsinki, Finland), which is, in principle, a computer-driven electro-microbalance (max. resolution 0.05 μN) that allows measurements to be made in the equilibrium or dynamic mode, advancing or receding. Test parameters (such as speed, immersion depth, and number of cycles), data acquisition (e.g., rate and trigger), and data reduction are all on-line software-controlled with possible postprocessing. For any liquid, tests were repeated at least five times, each run itself consisting of 10 cycles.

Dynamic Contact Angle Analysis

Contact angles on thin fibers are best determined as dynamic ones, i.e., advancing and receding, by the tensiometric method, the so-called micro-Wilhelmy technique. Other methods such as via the direct tangent are often not or only hardly suitable.[19] In principle, a single filament is suspended from a microbalance and then immersed (emersed) into (from) the test liquid by raising (lowering) the elevating stage with the test fluid reservoir. A schematic of the experimental setup is depicted in Figure 3.

The force excerted on the fiber may be expressed as the sum of wetting, gravitational, and buoyancy forces.[27] Therefore, the more general form of the Wilhelmy relationship[28] for the measured force F is given as

$$F = \gamma_l \pi D \cos \varphi + m_f g - \rho_l g y A_f \qquad (16)$$

and considers the weight in air of the fiber, usually tared out in the experiment, and the buoyancy force, which must be considered if there is anything other than zero immersion (D, A_f, and m_f are the fiber diameter, cross-sectional area, and mass, respectively; g represents the gravitational constant, ρ_1 stands for the density of the test liquid, and y is the immersion depth). Once these additional contributions are accounted for, the relationship is reduced to

$$F = \gamma_l \pi D \cos \varphi \qquad (17)$$

Since F, γ_l, and D are either known or independently evaluable, $\cos \varphi$ can be calculated from eq. (17). Although, here, no terms related to viscous effects are considered, it is satisfactory as wettability measurements are usually performed with low viscosity liquids.[29]

In detail, the filaments (max. 10 mm "free," unsuspended length) were mounted indirectly to a wire hook suspended from the measuring arm of the above-mentioned microbalance, trying to avoid any fiber damage or contamination. Then, after taring the balance, the liquid was raised until first contact with the fiber (setting of zero immersion depth) and, in order to exclude end effects, the fiber was immersed another 2 mm. By further moving the stage up to 9 mm fiber immersion depth and down again at a constant speed of 1 mm/min, typical F vs. y plots as given schematically in Figure 4 were recorded. The buoyancy effects were ruled out automatically (software) by extrapolation of the experimental traces within the given immersion depth range back to the zero value, whereby the first and last 1 mm of immersion are ignored. The intercepts of those extrapolation straights lines with the load axis yield the pure wetting forces F_a and F_r, where a means advancing and r receding, i.e., the immersion or emersion direction. Therefore, advancing (φ_a) and receding (φ_r) dynamic contact angles may be calculated from eq. (17). The apparent hysteresis

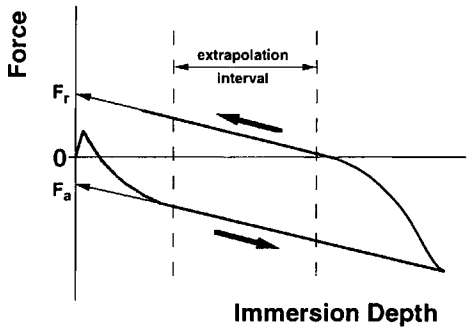

Figure 4 Wetting force–immersion depth–trace (1 cycle).

effect (see Fig. 4) may be explained by local surface inhomogeneity effects such as roughness and contaminants (e.g., Ref. 30) and is reported to be also velocity-dependent.[29] This results in the fact that it is obviously not easy to predict the stationary contact angle φ from φ_a and φ_r. Therefore, this value is defined, according to Ikada et al.,[30] via the arithmetic mean of their cosini, because these values are directly proportional to F_a and F_r [see eq. (17)]:

$$\cos \varphi = (\cos \varphi_a + \cos \varphi_r)/2 \qquad (18)$$

However, it is not clear whether or how φ correlates with the equilibrium contact angle θ. At least five tests of three cycles each were performed for all fiber/test liquid systems; one fiber was only contacted with one fluid in order to preclude artificial changes of the fiber surface chemistry and cross contamination of the test liquid.

CF/EP Droplet Formation

Contact angles α of cured epoxy resin droplets symmetrically formed on single filaments were examined by SEM applying the direct tangent method. As has been reported by Wu that these contact angles may be dependent on the droplet size,[19] only specimens were used where the fiber "embedded" (or microdroplet) length was similar, i.e., in the range between 40 and 50 μm. The average EP droplet angle α for each fiber type was determined using at least five specimens and all four individual angles each.

Micromechanical Composite Characterization

Single-fiber model specimens for the microdroplet pull-off tests were cured in a heating chamber (80°C/4 h + 120°C/8 h/oven-cooling), always using a vacuum-degassed EP resin. This testing technique, described, e.g., by Miller et al.[31] and schematically depicted in Figure 5, was performed using a specially designed and home-built microtensile testing machine equipped with highly precise load (full range: 1 N) and displacement (full range: 10 mm) transducers. This device allows the tests to be visually monitored by stereo light microscopy. Pull-out speed (0.5 mm/min) and fiber free lengths (7–8 mm) were kept constant in order to achieve similar conditions in terms of stored elastic energy (mainly in the fiber free length) for interface failure initiation and propagation. Load-displacement curves were monitored on an x-y plotter. Interfacial failure occurred when the applied force reached the maximum value F_{max} and dropped subsequently.

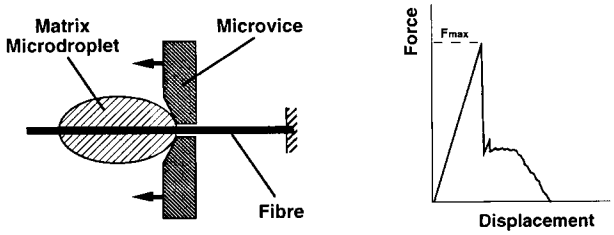

Figure 5 Microdroplet pull-off test.

The apparent interfacial shear strength IFSS (τ_i) value was calculated for at least 30 samples by

$$\tau_i = F_{max}/\pi DL \qquad (19)$$

where F_{max} is the maximum tensile load and D and L, the fiber diameter and embedded fiber length (determined by SEM), respectively.

To maintain the validity of this shear-stress criterion, tests were conducted on specimens where the embedded fiber lengths were considerably beneath 100 μm.[26] Microscopic observations *in situ* during the tests and typical force-displacement-traces as also depicted in Figure 5 indicated that interfacial failure occurred abruptly along the whole embedded fiber length—therefore, shear-stress-controlled.

Macromechanical Composite Characterization

Flat unidirectional laminate plates and hoop-wound tubular specimens were produced by wet filament winding of two rovings (12 k/800 tex) on a flat plate or a cylindrical mandrel, respectively. Their consolidation occurred in an autoclave (vacuum + 0.7 MPa) or a heating oven following the recommended curing cycle (80°C/4 h + 120°C/8 h/oven-cooling). More detailed information related to the fabrication and quality control of flat and tubular specimens is given by the authors in a recent publication.[26]

Tensile and torsion tests were carried out on tubular specimens using a tension/compression and torsion ("T/CT") Suter (Basel, Switzerland) universal testing machine. The strength values in transverse tension and shear gained by this testing technique are reported to be the most reliable material properties available.[26] Furthermore, transverse tensile tests on flat laminates were performed on edge-polished specimens according to the ASTM D 3039 standard; interlaminar shear strength (ILSS) was determined by short-beam shear testing (ASTM D 2344, support span-to-depth ratio of 4). All tests on laminate specimens were conducted on a Zwick 1474 universal testing machine.

Table I Comparison of Experimental Test Liquid Surface Tensions with the Literature Values

Test Liquid	Experimental: Wilhelmy γ_l (mN/m)	Experimental: DuNoüy γ_l (mN/m)	Literature: γ_l (mN/m)	Literature: γ_l^p (mN/m)	Literature: γ_l^d (mN/m)	Literature: $(\gamma_l^p/\gamma_l^d)^{0.5}$ (./.)	Data Reduction
Bromonaphthalene	42.7	43.9	44.6	0.0	44.6	0.00	O&W
Ethylene glycol/ formamide	50.5	49.6	50.5				ZIS
Formamide	58.0	58.1	58.3	26.0	32.3	0.90	ZIS
Glycerine	62.6	62.0	63.4	25.9	37.5	0.83	O&W/ZIS
Distilled water	71.1	70.4	72.8	51.0	21.8	1.53	O&W/ZIS

RESULTS AND DISCUSSION

Surface Tension of Test Liquids

In Table I, both literature values and experimental results are given for the test liquid surface free energies γ_l. Furthermore, it is indicated which liquid was used for which fiber surface free energy analysis method, i.e., either the Zisman (ZIS[25]) or the Owens and Wendt (O&W,[21] similar to Kaelble et al.[22]) wetting angle data reduction.

In summary, good correspondence turns out between the experimental techniques themselves (Wilhelmy plate and DuNouy ring methods), on the one hand, and the literature references (e.g., Ref. 24), on the other. For this confirmation of experimental results, and as the surface tension is tabulated in its polar and dispersive fractions, the literature values were used henceforth rather than the experimental ones.

Fiber Wetting and Surface Free Energy

Table II gives a survey of the dynamic contact angle measurement results φ for the Idemitsu (variation of surface treatment level) and the Tenax (variation of surface treatment and/or surface finish) CF types. It should be noted again that the contact angles listed here were calculated from the advancing and receding ones following eq. (18). Additionally, the average contact angles α of EP (the surface free energy often reported in literature for EP in the solid state $\approx$ 47 mN/m; here, experimentally measured for the liquid state $\approx$ 42 mN/m) in cured microdroplet pull-off specimens are summarized.

In general, there is a global tendency toward smaller contact angles with increasing surface treatment level and decreasing test liquid surface tension for the Idemitsu fibers to be recognized. For the Tenax ones, the untreated 5000 differs clearly from the standard surface treated 5001 and 5411, which correlate quite well. The 5411B modification yields the largest φ values, what is indicative of the possible fiber/liquid interactions being minimized by surface coating, whereas the EP-coated 5131 exhibits the smallest φ, at least for higher γ_l.

The microdroplet contact angle α decreases with increasing surface treatment level and also with EP sizing; it exhibits its maximum for the fiber surface active sites being blocked by the release agent coat-

Table II Survey of Dynamic Contact Angles and Cured Epoxy Microdroplet Angles

Dynamic Contact Angle φ (deg)	Idemitsu (Surface Treatment Level): No	Mild	Usual	Severe	Tenax HTA (Surface Finish): 5411B	5000	5001	5411	5131
Bromonaphthalene	37.3	33.7	32.9	32.4	49.0	47.4	48.8	47.7	52.0
Ethylene glycol/ formamide	—	—	—	—	49.4	42.3	35.1	33.3	—
Formamide	57.7	46.2	41.5	30.3	61.0	55.8	47.2	48.6	34.9
Glycerine	60.7	54.9	48.3	40.2	68.2	62.5	54.1	52.7	46.0
Distilled water	79.4	70.0	66.5	57.4	83.6	77.0	69.5	67.9	56.9
EP droplet contact angle (cured) α (deg)	50.0	47.5	45.0	41.0	58.3	48.5	45.5	45.5	41.5

ing. In Figures 6(a) and (b) and 7(a) and (b), the wetting angle data reduction methods as proposed by Owens and Wendt (Fig. 6) and by Zisman (Fig. 7) have been applied to the wetting data sets gained for the Idemitsu (a) and Tenax (b) fibers. Referring to the O&W method in Figure 6, it is obvious that the wetting data points for each fiber type coincide quite well with a straight line, the least-squares linear fit of which is also given by the equation. Its y-axis intercept (measure for γ_s^d) remains hardly affected within each fiber series, but the slope (measure for γ_s^p) increases with increasing surface treatment level or EP-sizing. Figure 7 depicts the ZIS plots for both fiber types, whereby, again, a least-squares linear fit was successfully applied to the experimental wetting data. Here, the fiber total surface free energy γ_s is identified with the critical surface tension γ_c (or γ_l^*) for which cos φ is 1. Variation of the surface-treatment level and/or sizing results in a band of more or less parallel interpolation straights, and γ_c increases with increasing surface treatment level and EP sizing.

All the results in terms of fiber total surface free energy and its polar and dispersive fractions as determined by the ZIS and the O&W methods, respectively, are summarized in Table III. Here, it is noteworthy that both data-reduction methods reveal quite similar results, although γ_{sl} is neglected by Zisman [see eq. (8) for Owens and Wendt]. An increasing surface treatment level generally yields higher fiber surface free energies (Idemitsu), and coating of standard surface-treated Tenax HTA fibers with the release agent (5411B) or EP sizing (5131) results in a minimized or maximized γ_s value. Apparently, since $\gamma \approx 47$ mN/m for epoxy, the EP size was measured for the 5131 modification rather than for the fiber surface itself. Both untreated types, i.e., Idemitsu "no treatment" and Tenax HTA 5000, do not differ significantly in surface free energy. Nevertheless, Idemitsu's "usual" treatment (ca. 48 mN/m) exceeds the standard surface treatment as applied by Tenax Fibers (ca. 42 mN/m) considerably. This might either be a hint for a higher degree of crystallinity for the Tenax fiber or a more intensive surface treatment technique used by Idemitsu. However, "standard level" surface treatment of the untreated fibers seems to result in an only moderately enlarged surface tension (Idemitsu: ca. 19%, Tenax: ca. 16%) if compared to the full "severe treatment" potential (ca. 27%).

By splitting up the fiber surface total free energies into their polar and dispersive contributions, it be-

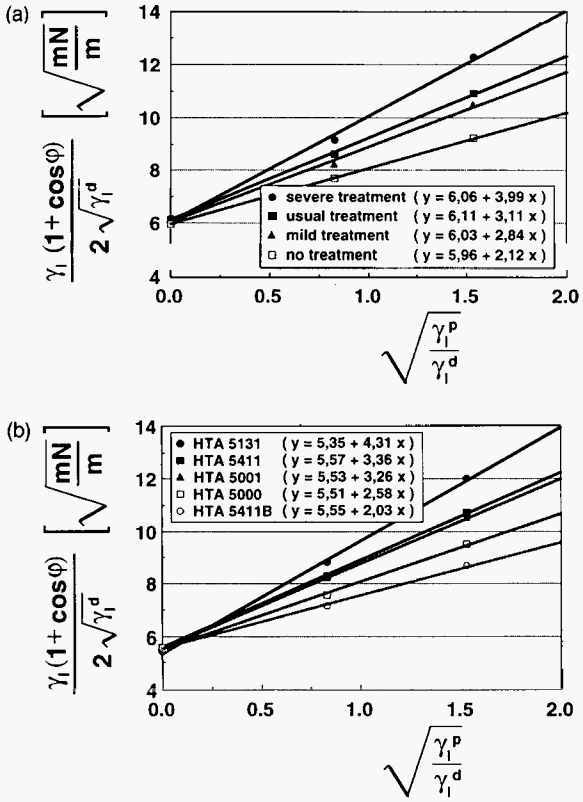

Figure 6 O&W plots for (a) Idemitsu and (b) Tenax fibers.

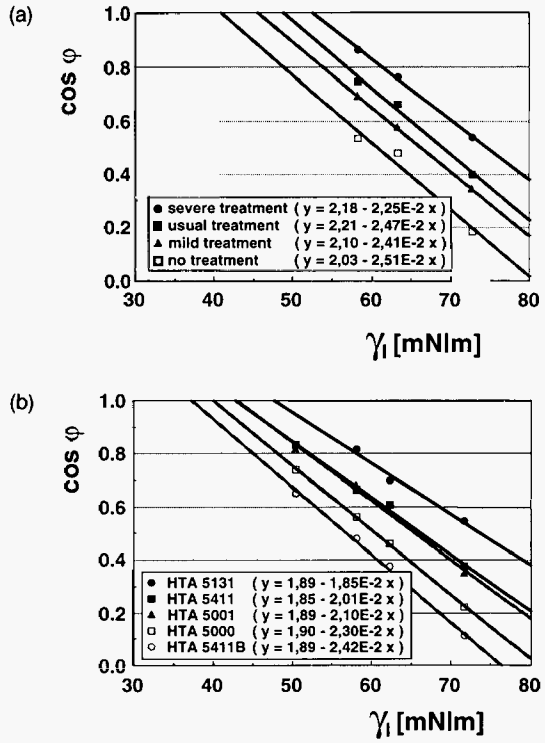

Figure 7 Zisman plots for (a) Idemitsu and (b) Tenax fibers.

Table III Summary of Polar, Dispersive, and Fiber Total Surface Free Energies

Fiber Surface Free Energy (mN/m)	Idemitsu (Surface Treatment Level)				Tenax HTA (Surface Finish)				
	No	Mild	Usual	Severe	5411B	5000	5001	5411	5131
Total surface free energy γ_s (ZIS)	41.0	45.6	48.8	52.2	36.7	39.3	42.6	42.2	47.9
Total surface free energy γ_s (O&W)	40.1	44.5	47.1	52.6	34.9	37.0	41.1	42.3	47.2
Polar surface free energy γ_s^p (O & W)	4.5	8.1	9.7	15.9	4.1	6.7	10.6	11.3	18.6
Dispersive surface free energy γ_s^d (O&W)	35.6	36.4	37.4	36.7	30.8	30.3	30.5	31.0	28.6

comes obvious that both the Idemitsu and the Tenax surface-treatment techniques result primarily in an increase of the polar fraction of the surface tension γ_s^p, whereas its dispersive part γ_s^d remains hardly affected. In comparing the Idemitsu fiber types with the Tenax ones, it turns out, on the whole, that the former exhibit ca. a 5–6 mN/m higher γ_s^d level than that of the latter and that "usual" (Idemitsu) and standard (Tenax HTA 5001, 5411) surface treatment are nearly similar in γ_s^p, the Tenax types showing negligibly higher values. As the original γ_s^p level for the untreated fibers is slightly higher for the Tenax HTA 5000 (γ_s^p = 6.7 mN/m) type than for the Idemitsu one without surface treatment (γ_s^p = 4.5 mN/m), the "usual" (Idemitsu) and standard treatment levels (HTA 5001) result in an increase of γ_s^p by 115% (!) and 58%, respectively. Nevertheless, if polar interactions are mainly responsible for CF adhesion to EP—as proposed in the relevant literature reviewed earlier in this article—the standard Tenax surface treatment should be as efficient as is the Idemitsu "usual" one. It should further be mentioned that γ_s^d cannot be influenced by release agent fiber coating (5411B), but γ_s^p is dramatically minimized. HTA 5131 differs from the rest of the Tenax series as EP (sizing) is actually analyzed.

Micromechanical Composite Characterization

The interfacial shear strength values IFSS for all fiber types are summarized in Table IV. It can easily be concluded that the fiber/matrix adhesion as determined in the microdroplet pull-off test is enhanced by the intensification of fiber-surface treatment. So, "mild," "usual," and "severe" surface treatments of the untreated Idemitsu fibers do gradually increase the IFSS by 20%, 31%, and 52%, respectively. As can be concluded from these results,

Table IV Survey of Macro- and Micromechanical Strength Properties

Strength (MPa) (Specimen Type)	Idemitsu (Surface Treatment Level)				Tenax HTA (Surface Finish)				
	No	Mild	Usual	Severe	5411B	5000	5001	5411	5131
Interfacial shear strength (IFSS) (model specimen)	42.5 ± 3.8	51.1 ± 2.2	55.7 ± 2.2	64.7 ± 4.2	18.5 ± 1.5	45.8 ± 1.8	55.4 ± 2.1	55.7 ± 1.6	71.7 ± 2.1
Interlaminar shear strength (ILSS) (laminate specimen)	—	—	—	—	44.0 ± 2.3	—	—	65.0 ± 2.7	79.5 ± 2.0
"Torsion shear strength" (TSS) (tube specimen)	—	—	—	—	53.5 ± 0.8	—	—	71.2 ± 0.3	70.3 ± 1.6
Transverse tensile strength (laminate specimen)	—	—	—	—	15.2 ± 3.0	—	—	23.8 ± 4.2	33.3 ± 4.4
Transverse tensile strength (tube specimen)	—	—	—	—	20.7 ± 0.8	—	—	48.8 ± 0.5	53.1 ± 3.5

there is no hint for removal of a weak outer carbon fiber surface layer resulting in a considerable—if compared to more severe treatment—increase of IFSS for initial treatment of an untreated fiber.[3,9]

Tenax's proprietary standard surface treatment (5001, 5411) enhances the IFSS by ca. 21% with respect to the untreated HTA 5000 variant. Adhesion to epoxy can further be improved (57%) by an EP size (HTA 5131) and minimized, however, by coating the fiber with the release agent (HTA 5411B). The results for the chemically blocked standard surface-treated fiber are unambiguously indicative of the fiber/matrix interactions—for this particular CF/EP system studied—being mainly of a chemical nature rather than due to surface roughness-induced mechanical interlocking. The latter phenomenon was proposed by Drzal et al., e.g., in Ref. 3 or Ref. 9, and is based on comparative studies with untreated, treated, and treated + selectively blocked surface active groups.

A direct correlation between the IFSS, on the one hand, and the polar fraction of the fiber surface free energy γ_s^p, on the other, is confirmed (a) by the identity of IFSS values for fibers of similar γ_s^p (Idemitsu "usual" and Tenax HTA 5001 and 5411) and (b) by slightly higher IFSS for the untreated Tenax HTA 5000 in comparison with the Idemitsu "no treatment" variant.

Macromechanical Composite Characterization

The results of the macromechanical tests performed on Tenax HTA 5411B/EP, HTA 5411/EP, and HTA 5131/EP flat laminate and tubular unidirectional composites, i.e., the strength properties in transverse tension and shear given by their mean value ± standard deviation are listed in Table IV. It is striking at first sight that there occur significant differences in the strength properties not only between shear and transverse tensile testing methods, but also in between each of them. Anyway, it should be noted here that the strength levels found correspond quite well with those reported for composite laminates[32] and tubular specimens[33] of comparable composite systems.

Concerning the composites' transverse tensile strength, the influence of the interface turns out distinctly: HTA 5131 yields maximum strength, whereas HTA 5411B CF exhibits minimum adhesion to the EP matrix. The interfacial bond quality of the 5411 variant lies in between those of the two aforementioned modifications. However, the strength values gained from tests conducted on tubular specimens exceed those ones determined by flat laminate tensile testing. Referring to the shear properties, the short beam shear (SBS) test method differentiates clearly between the interfacial bond qualities, whereas the tube torsion test results in similar strength values for the HTA 5131 and the HTA 5411 CF/EP variants and in a slight deterioration for the HTA 5411B/EP version.

These results have been discussed recently by the authors in a more comprehensive study on interfacial effects in off-axis composite mechanical properties.[26] In conclusion and as far as uniaxial test methods are considered, only torsion and transverse tensile testing of tube specimens seems to yield reliable strength values that can be considered as material parameters.

These values are generally superior to those derived from the laminate tests due to a "purer" uniaxial stress state accommodated. Tests on flat laminates, on the other hand, yield controversial results. It is likely, therefore, that failure in both transverse and shear testing of laminates is initiated by stress concentrations (due to clamping, loading, or other imperfections, and inherent material notch sensitivity effects). These turn out to be strictly related to the interfacial bond quality itself.

Effects of Surface Energetics on Wetting and Adhesion Properties

As already mentioned under Micromechanical Composite Characterization, there was a linear correlation found between the interfacial shear strength IFSS as determined by microdroplet pull-off testing and the polar fraction of the surface free energy γ_s^p. This result is graphically depicted and given by equation in Figure 8(a) and (b) for both (a) the Idemitsu and (b) the Tenax fiber series. Linear relationships could also be determined between IFSS and γ_s, the total fiber surface free energy. But that is trivial, because the dispersive contribution γ_s^d remains nearly unchanged for varied surface treatments. These findings are consistent with those reported by Drzal et al.,[34] Mäder et al.,[35] and Krekel et al.[10] In the following, it will be shown by experimental data that such a linear approximation is indeed reasonable:

(i) Recalling eq. (11) for the determination of fiber surface free energy dispersive and polar fractions according to the O&W method, the latter one is determined by the slope of the straight-line fit. Assuming (a) that the apparent microdroplet angles α formed by wetting of the filaments are also indicative

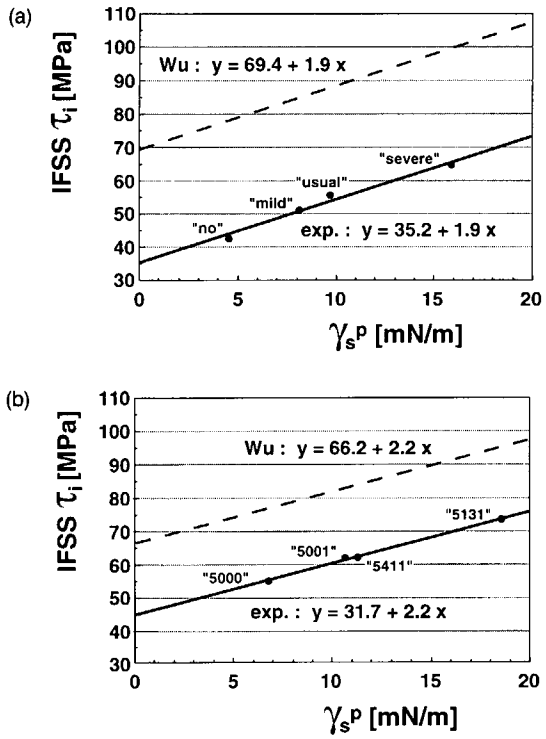

Figure 8 IFSS–γ_s^p plots for (a) Idemitsu and (b) Tenax fibers.

of the polar fiber/matrix interactions present and thus a measure for γ_s^p and (b) that these angles are not changed due to EP resin curing, it may be concluded that a relation between α and γ_s^p can also be described by eq. (11). Since γ_l is constant for the epoxy used and as γ_s^d is hardly influenced by surface treatment within each fiber series, eq. (11) rearranges to

$$1 + \cos \alpha = A(\gamma_s^p)^{0.5} + B \qquad (20)$$

where A and B are constants with $A = 2\{(\gamma_l^p)^{0.5}/\gamma_l\}$ and $B = 2\{(\gamma_l^d\gamma_s^d)^{0.5}/\gamma_l\}$. Therefore, γ_s^p is given by a polynom of second order in cos α. The results of the inverted correlation, i.e., cos α in function of γ_s^p, are depicted graphically and given by equation for the least-squares fit curves in Figure 9(a) and (b) for the (a) Idemitsu and (b) Tenax fibers. It becomes clear by considering the order of the coefficients in x^2 that the curves are linear in good approximation for the γ_s^p interval of interest.

(ii) There was also a linear relationship found between the IFSS and cos α for the CF/EP microdroplet pull-off specimens. These results are given in Figure 10(a) and (b) for (a) Idemitsu and (b) Tenax fiber material.

In conclusion from (i) and (ii), i.e., the linear relationship between cos α and γ_s^p, on the one hand, and between IFSS and cos α, on the other, it may be deduced that there exists a linear correlation between IFSS and γ_s^p.

Concerning the Tenax HTA fibers [Fig. 8(b)], one has to realize that the 5411B modification does not fit the least-squares linear fit at all. This was a priori to be expected, because the release agent coating was applied to hinder chemical interactions between the fiber surface and matrix resin reactive groups, thus revealing a completely different interface chemistry (it should be noticed that the Tenax HTA 5411B modification was left out in the above considerations for this reason). Therefore, the slope of such a straight-line fit should be given by the kind and number of the chemical bond present, as far as its type remains the same. This restriction is met for all fiber variants (exception: 5411B), since mainly C—O or C—C (nearly identical binding energies) will form with the epoxy matrix resin. As an EP sizing is usually nothing else but neat epoxy, the same is also valid for the coated Tenax HTA 5131. The relation between the chemical bond and IFSS

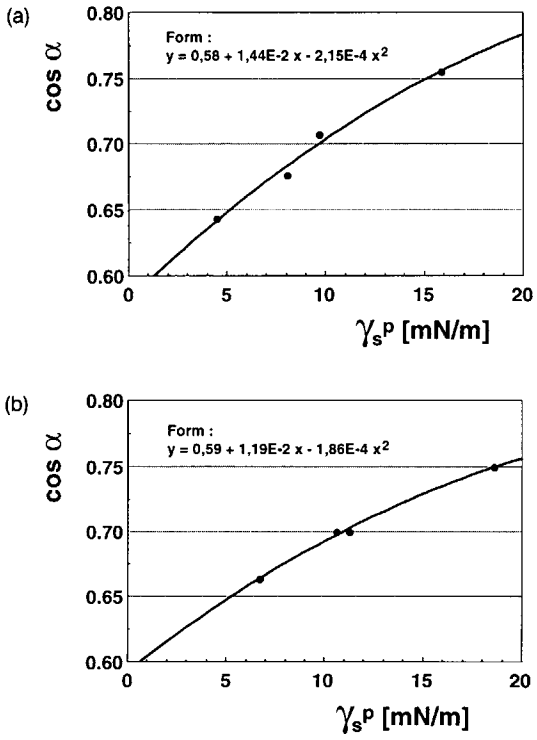

Figure 9 cos α–γ_s^p plots for (a) Idemitsu and (b) Tenax fibers.

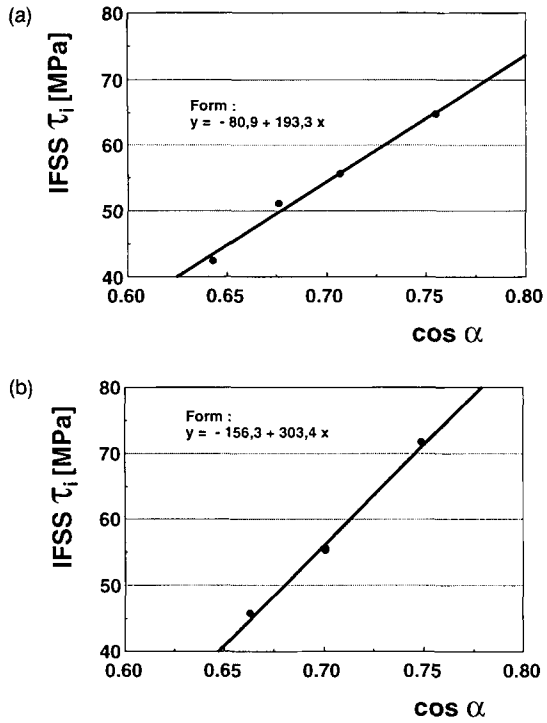

Figure 10 IFSS–cos α plots for (a) Idemitsu and (b) Tenax fibers.

as postulated above can be confirmed by the "quasi-similarity" of the line fit slopes (measure for the efficiency of the chemical bond) for the Idemitsu- and Tenax-type fibers. However, it is not clear which information will be provided by the straight-line intercept exactly, but it should be indicative of an adhesion level due to dispersive fiber/matrix interactions (van der Waals forces, absence of functional groups, $\gamma_s^p = 0$) and mechanical interlocking. The latter itself must be dependent on the direction of fiber/matrix separation, i.e., parallel (shear) or perpendicular (transverse tension) to the fiber axis. So, the test method as well as the relevant matrix stiffness (Young's modulus E or shear modulus G) will be of considerable influence, as well.

Some mechanical parameters are taken into account in the "wetting and interfacial defect" model proposed by Wu, but these considerations are based on the Griffith fracture mechanical problem (see Wetting and Interfacial Defect section) and thus not directly applicable to the microdroplet pull-off test.

Anyway, eq. (14) may be rewritten as in the following, because γ_s^d is approximately constant:

$$\tau_i = K\gamma_s^p + C \tag{21}$$

So, if K is the slope (determined by the type of chemical bond) of the fit straight line in the γ_s^p–IFSS plots depicted in Figure 8(a) and (b), the intercept C should be equal ($K\gamma_s^d$). This is not the case, neither for the Idemitsu (average $\gamma_s^d \approx 36.5$ mN/m) nor for the Tenax (average $\gamma_s^d \approx 30.1$ mN/m) fiber series, but, systematically,

$$C \approx \frac{K\gamma_s^d}{2} \tag{22}$$

Therefore, the linear relationship experimentally found for γ_s^p and the IFSS as determined in the microdroplet pull-off test is

$$\tau_i \approx K(\gamma_s^p + \gamma_s^d/2) \tag{23}$$

It must be noted here that this semiempirical equation is claimed only to be valid for this particular testing technique performed, but it should be generally applicable to comparable CF/EP systems, because the chemical fiber/matrix bond types will be the same. Further work has to scope the influence of the testing technique to prove the hypothesis that only the IFSS–γ_s^p intercept will be affected (at least for the type of interface loading kept constant), i.e., the microdroplet pull-off test results will be compared with other micromechanical test methods such as single-fiber fragmentation.

Referring to the macromechanical transverse tensile and shear tests, there turns out to be a linear relationship between the strength values found and the corresponding IFSS (see Fig. 11) for the Tenax HTA 5411B, 5411, and 5131/EP composite systems. But this is not the case for torsion testing of tubular specimens, although torsion and transverse tensile testing of tubes is proposed to yield most versatile strength values.[26] However, there is no direct 1 : 1

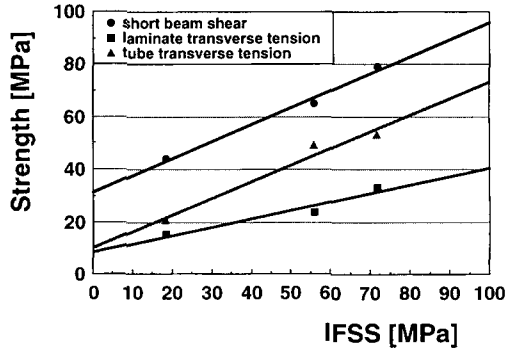

Figure 11 Correlation of macro- and micromechanical strength properties for Tenax fibers.

relation to be determined. Attempts to correlate γ_s^p with "strength" values were left out because 5411B/EP's interface chemistry is uncomparable with the 5411 and 5131 modifications (see above).

CONCLUSIONS

To determine the effect of surface treatment and/or sizing on both the individual fiber-surface properties and the mechanical performance of composites, two series of PAN-based high-tenacity CFs only varying in their surface-treatment intensity and/or kind of sizing were investigated for their wetting behavior and selected composite mechanical properties. For the latter, a hot-curing epoxy resin served as the composite matrix material.

Surface free energies for the CFs were determined by dynamic contact angle measurements in a variety of test liquids of known polar and dispersive surface-tension components utilizing a micro-Wilhelmy balance and following the wetting data reduction methods proposed by Zisman and Owens and Wendt, respectively. Both approaches yield similar results for the respective total surface free energy. Further partitioning into its polar and dispersive components indicates for both fiber series that the kind of surface treatment applied results in an increase of the polar fraction of the surface free energy, whereas the dispersive part remains hardly affected.

It can easily be concluded from the interfacial shear strength values as determined in the microdroplet pull-off test that the fiber/matrix adhesion is enhanced by both the intensification of fiber-surface treatment and coating the fiber with an EP sizing. Furthermore, there is no hint for removal of a weak outer CF surface layer by initial treatment of an untreated fiber. A direct correlation between the IFSS and the polar fraction of the fiber surface free energy γ_s^p is evidenced by the identity of IFSS values for fibers of similar surface tension polar contribution. Considering the fiber contact angles α of cured microdroplet specimens, it may be deduced from the linear relationships found between $\cos \alpha$ and γ_s^p, on the one hand, and between IFSS and $\cos \alpha$, on the other, that there exists a global linear correlation between IFSS and γ_s^p. A semiempirical equation based on fracture mechanical considerations related to the interdependency between wetting and interfacial defects has been proposed to determine IFSS in function of γ_s^p and γ_s^d.

Referring to the macromechanical transverse tensile and shear tests, a linear relationship between strength values and the corresponding IFSS composite systems turns out for all test methods with the exception of tensile testing of tubular specimens.

Financial support of this work by the Deutsche Forschungsgemeinschaft (DFG FR 675/13-1, "Interface Effects") and the Deutscher Akademischer Austauschdienst (DAAD/ARC) is gratefully acknowledged. Thanks are due to Idemitsu Kosan (Chiba, Japan), Tenax Fibers (Wuppertal, Germany), Ciba (Basel, Switzerland), and ACMOS Chemicals (Bremen, Germany) for providing materials.

REFERENCES

1. A. B. Pangelinan, R. L. McCullough, and M. J. Kelley, *J. Thermoplast. Compos. Mater.*, **7,** 192 (1994).
2. G. Krekel, K. J. Hüttinger, W. P. Hoffmann, and D. S. Silver, *J. Mater. Sci.*, **29,** 2968 (1994).
3. L. T. Drzal, N. Sugiura, and D. Hook, in *Proceedings of the American Society for Composites—Ninth Technical Conference,* Technomic, Lancaster, 1994, p. 1001.
4. W. W. Wright, *Compos. Polym.*, **3,** 231 (1990).
5. P. Marshall and J. Price, *Composites,* **22,** 388 (1991).
6. J. Matsui, *Crit. Rev. Surf. Chem.*, **1,** 71 (1990).
7. J. D. H. Hughes, *Compos. Sci. Technol.*, **41,** 13 (1991).
8. M. Guigon and E. Klinklin, *Composites,* **25,** 534 (1994).
9. L. T. Drzal, M. J. Rich, and P. F. Lloyd, *J. Adhes.*, **16,** 1 (1982).
10. G. Krekel, U. J. Zielke, K. J. Hüttinger, and W. P. Hoffmann, *J. Mater. Sci.*, **29,** 3984 (1994).
11. F. Nakao, Y. Takenaka, and H. Asai, *Composites,* **23,** 365 (1992).
12. C. Jones, *Compos. Sci. Technol.*, **42,** 275 (1991).
13. E. Fitzer and R. Weiss, *Carbon,* **25,** 455 (1987).
14. G. Krekel, K. J. Hüttinger, and W. P. Hoffmann, *J. Mater. Sci.*, **29,** 3461 (1994).
15. L. T. Drzal, M. J. Rich, M. F. Koenig, and P. F. Lloyd, *J. Adhes.*, **16,** 133 (1982).
16. W. W. Wright, *Compos. Polym.*, **3,** 360 (1990).
17. T. H. Cheng, J. Zhang, S. Yumitori, F. R. Jones, and C. W. Anderson, *Composites,* **25,** 661 (1994).
18. P. I. Marshall, D. Attwood, and M. J. Healey, *Composites,* **25,** 752 (1994).
19. S. Wu, *Polymer Interface and Adhesion,* Marcel Dekker, New York, 1982.
20. A. H. Gilbert, B. Goldstein, and G. Marom, *Composites,* **21,** 408 (1990).
21. D. K. Owens and R. C. Wendt, *J. Appl. Polym. Sci.*, **13,** 1741 (1969).
22. D. H. Kaelble, P. J. Dynes, and E. H. Cirlin, *J. Adhes.*, **6,** 23 (1974).
23. F. M. Fowkes, in *Chemistry and Physics of Interfaces,* American Chemical Society, Washington, DC, 1965, p. 1.
24. G. E. Hammer and L. T. Drzal, *Appl. Surf. Sci.*, **4,** 340 (1980).

25. W. A. Zisman, in *Contact Angle, Wettability and Adhesion,* R. F. Gould, Ed., Advances in Chemistry Series 43, American Chemical Society, Washington, DC, 1964, p. 1.
26. F. Hoecker, K. Friedrich, H. Blumberg, and J. Karger-Kocsis, *Compos. Sci. Technol.,* **54,** 317 (1995).
27. M. Weinberg, in *Toughened Composites, ASTM STP 937,* N. J. Johnston, Ed., American Society for Testing and Materials, Philadelphia, 1987, p. 166.
28. B. Miller, L. S. Penn, and S. Hedvat, *Colloids Surf.,* **6,** 49 (1983).
29. G. Giannotta, M. Morra, E. Occhiello, F. Garbassi, L. Nicolais, and A. D'Amore, *Compos. Manuf.,* **3,** 59 (1992).
30. Y. Uyama, H. Inoue, K. Ito, A. Kishida, and Y. Ikada, *J. Colloid Interf. Sci.,* **141,** 275 (1991).
31. B. Miller, P. Muri, and L. Rebenfeld, *Compos. Sci. Technol.,* **28,** 17 (1987).
32. L. T. Drzal and M. Madhukar, *J. Mater. Sci.,* **28,** 569 (1993).
33. R. Schröder, R. Schmid, and M. Raetzo, in *Plastics-Metals-Ceramics,* H. L. Hornfeld, Ed., SAMPE European Chapter, Switzerland, 1990, p. 395.
34. L. T. Drzal, M. Madhukar, and M. C. Waterbury, *Compos. Struct.,* **27,** 65 (1994).
35. E. Mäder, K. Grundke, H.-J. Jacobasch, and G. Wachinger, *Composites,* **25,** 739 (1994).

Received February 11, 1995
Accepted June 25, 1995